

## Supplementary Information

The detailed characteristics methods are displayed as follows (Section S1).

Powder X-ray diffraction patterns (XRD) were measured on a Bruker D8 advance powder diffraction system using Cu K $\alpha$  ( $\lambda = 1.5408 \text{ \AA}$ ). The morphology and structure of samples were examined by scanning electron microscope (SEM) (Regulus8100). Fourier transform infrared (FT-IR) spectra were measured on a Nicolet iS10 spectrophotometer (Thermo Field USA) in the range of 4000 to 400  $\text{cm}^{-1}$  with a resolution of 2  $\text{cm}^{-1}$ . The nitrogen adsorption-desorption isotherm of the photocatalyst was measured using the ASAP2010C surface pore adsorption instrument (Micromeritics Instruments, USA), and the corresponding specific surface area and related pore size data of the catalyst were obtained at a testing temperature of 77 K. Then, based on the existing aperture data, use Nano measurer software to draw an aperture distribution map. The X-ray photoelectron spectra (XPS) of samples were characterized by ESCALAB 250xi with Al K $\alpha$  radiation at 1486.6 eV. The optical measurements were carried out by UV-Vis spectrophotometer (Shimadzu UV-160 A) in mode DRS in the wavelength range of 200-800 nm and PL spectrometer on Agilent G9800A analyzer. The electrochemical properties of catalysts were analyzed by linear sweep voltammetry (LSV) and electrochemical impedance spectrum (EIS) on an electrochemical workstation (PP211, Zahner Co., Germany) using conductive glass electrode coated with catalyst powder as the working electrodes and using 0.5 M Na<sub>2</sub>SO<sub>4</sub> as the bath solution. Electron paramagnetic resonance (EPR) spectroscopy measurements were obtained on a Bruker A300 with Microwave Bridge (microwave frequency, x-band; microwave power, 18.8 mW; modulation amplitude, 1 G; modulation frequency, 100 KHz) at room temperature. Analysis of the intermediates of the photocatalytic degradation process was performed by an HPLC-MS Spectrometer (LC-MS, Waters Alliance 2695) equipped with an electrospray ionization (EI) source.

The process of ion exchange reaction between phosphotungstic acid and LDHs are displayed as follows (Section S2).

When phosphotungstic acid solution was mixed with NiFe-LDHs suspension, the phosphotungstic acid anion began to approach the layered structure of NiFe-LDHs. Due to the existence of exchangeable anions (such as carbonate, nitrate, etc.) in the NiFe-LDHs layer, the phosphotungstate anion will adsorb on the surface of NiFe-LDHs and try to enter the interlayer. Under the conditions of stirring and pH adjustment, the phosphotungstic acid anion was exchanged with the original anion between the NiFe-LDHs layer. This process is usually accomplished through a combination of

electrostatic action, steric hindrance effect, and interlayer water molecules. As a result of the exchange reaction, the phosphotungstate anion successfully enters the NiFe-LDHs interlayer, while the original anion is released into the solution. After the ion exchange reaction, phosphotungstate anions stably exist between the NiFe-LDHs layers, forming LDHs complexed intercalated by phosphotungstic acid. This complex combines the high catalytic activity of phosphotungstic acid with the layered structure advantage of LDHs, which may have better performance.

The specific research methods and details of the experimental section are as follows (Section S3).

## 1. Determination of influencing factors

### (1) The influence of inorganic ions

Add aqueous solutions containing  $\text{Cl}^-$ ,  $\text{CO}_3^{2-}$ ,  $\text{Fe}^{2+}$ , and  $\text{Ca}^{2+}$  uniformly into beakers (50mL) containing 30mg/L tetracycline hydrochloride (TC-HCl) pollutant solution and 30mg catalyst (PTA-LDHs), and label them as experimental groups. Mark the beaker containing only catalyst and pollutants as the control group for photocatalytic degradation experiments. Compare the removal efficiency of two groups of pollutants and explore the influence of inorganic ions on catalytic performance.

### (2) The impact of humic acid (HA)

Prepare humic acid aqueous solutions with concentrations of 5 and 20 mg/L, and evenly add them to a beaker containing pollutants containing catalysts as the experimental group. Compare with a beaker containing only catalysts and pollutants. Compare the removal efficiency of two groups of pollutants and explore the impact of HA on catalytic performance.

### (3) The impact of different water qualities

Collect deionized water, alkaline mineral water, tap water, factory wastewater, and domestic wastewater, prepare them into a pollutant solution containing 30 mg/L (TC-HCl), add catalysts (PTA-LDHs), and conduct photocatalytic degradation experiments.

### (4) The impact of different pollutants

Select three antibiotics, such as oxytetracycline (OTC), furantoin (NFT), and naproxen (NPX), and prepare them into a 30 mg/L pollutant solution. Add catalysts for photocatalytic degradation experiments to study the broad-spectrum properties of PTA-LDHs.

## 2. Determination of intermediate products

Using ACQUITY UPLC BEH C18 chromatography column (1.7 using UPLC-MS system  $\mu\text{m}$ .  $2.1 \times 50$  mm) and quadrupole time-of-flight mass spectrometer

(Waters Synapt G2, USA) including ESI electric spray ion source. Mobile phase A is acetonitrile, and mobile phase B is 0.1% formic acid. Use binary mobile phase at a flow rate of 0.3 mL/min. The mobile phase gradient is set to A=5% (0 min), 17% (5 min), 30% (7 min), 85% (11 min), 100% (13 min), 5% (14 min), and 5% (20 min). The injection volume is 5.0  $\mu$  L. The identification of products is based on retention time and mass spectrometry. The capillary voltage is 3.0 kV, the cone hole voltage is 40 V, and the extraction cone voltage is 4.0 V. The ion source temperature and solvent removal temperature are 373 K and 623 K, respectively. The gas velocity in the conical hole is 50 L/h, and the solvent gas removal rate is 700 L/h. The full scan quality range is 100 to 1000 m/z.

The specific test method of electrochemical impedance spectroscopy (EIS) is as follows (Section S4).

Electrochemical impedance spectroscopy (EIS) curves were collected with the range of 0.1 to 100000 Hz and the amplitude of 5 mV at specific voltage of 160 mV. Stability was measured through the 2000 CV cycle in acidic and alkaline solutions and i-t curves acquired by chronograph amperage at constant operating voltage over 24 h.

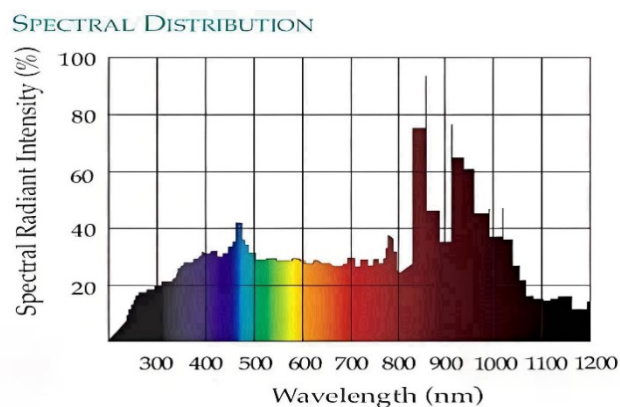


**Fig. S1** Spectrum of xenon lamp

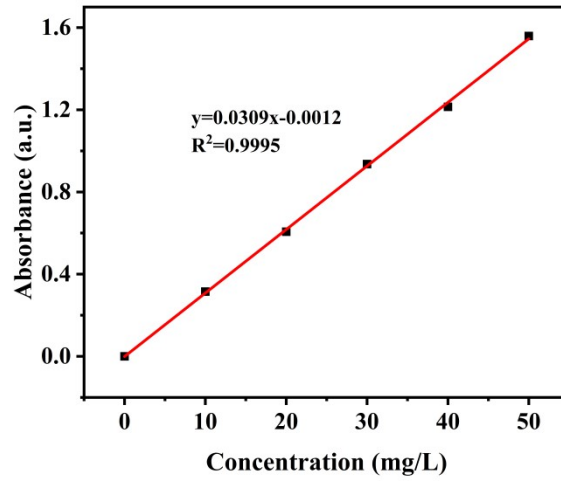


**Fig. S2** Standard curve of TC-HCl.

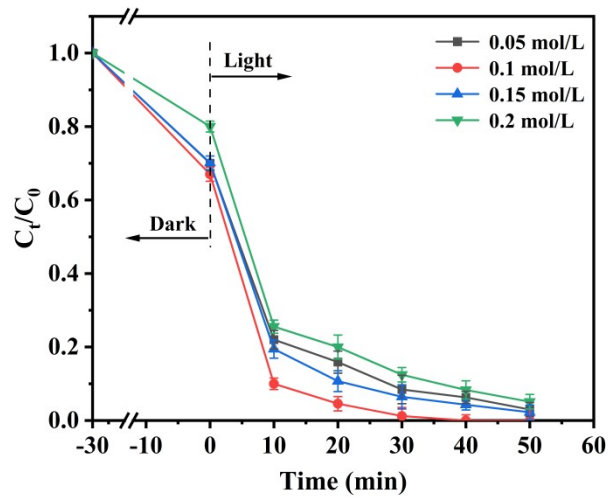


**Fig. S3** The effect of amount of phosphotungstic acid doped on the removal of TC-HCl.

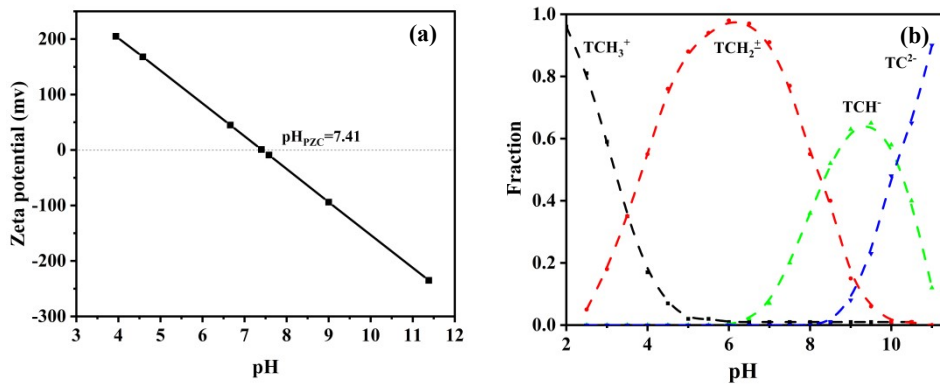


**Fig. S4** The isoelectric point of PTA-LDHs (a); The morphology of TC-HCl at different pH (b).

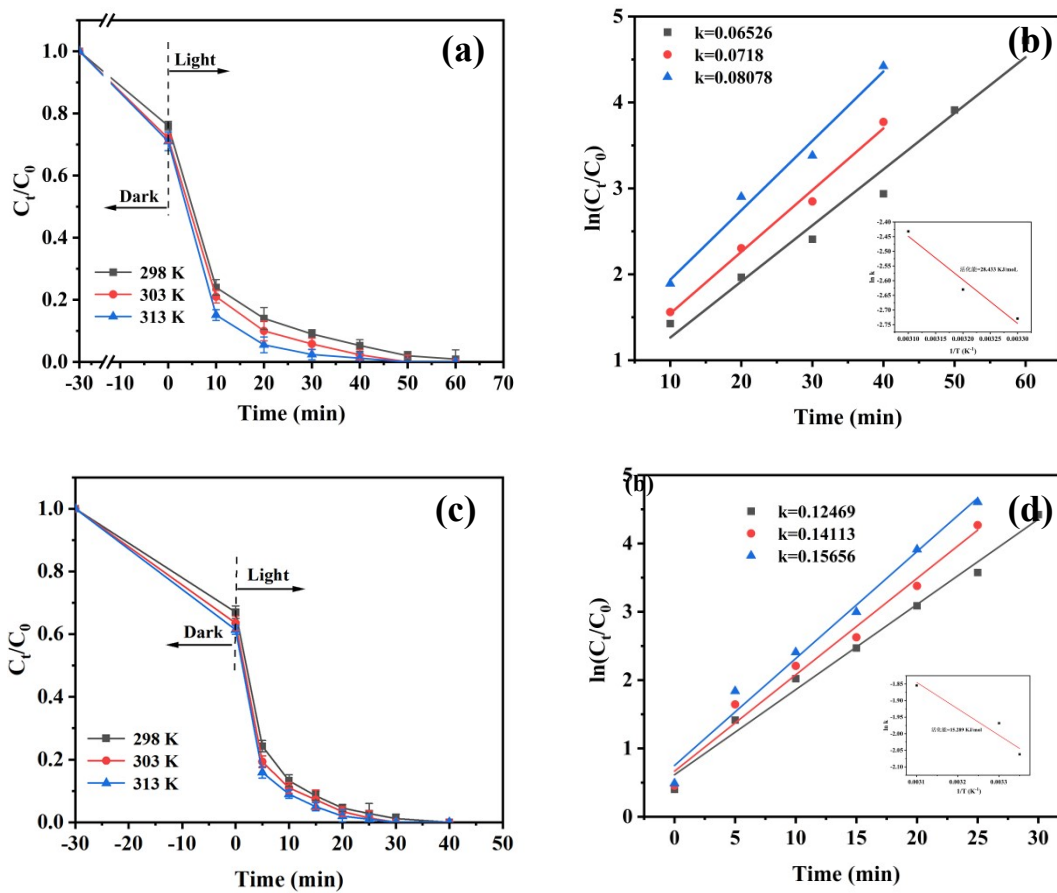


**Fig. S5** Effects of NiFe-LDHs LDH (a, b) and PTA-LDHs (c, d) on TC-HCl degradation at different reaction temperatures and the corresponding kinetic fitting curves.

**Fig. S6** (a) SEM image; (b) XRD; (c) FT-IR; (d) total XPS spectrum before and after reaction.

(a)

(b)

(c)

(d)

(c)

(d)

**Fig. S7** (a) UV-vis DRS and Tauc-plot; (b) LSV curves; (c) EIS nyquist plots; (d) PL spectra of NiFe-LDHs and PTA-LDHs.

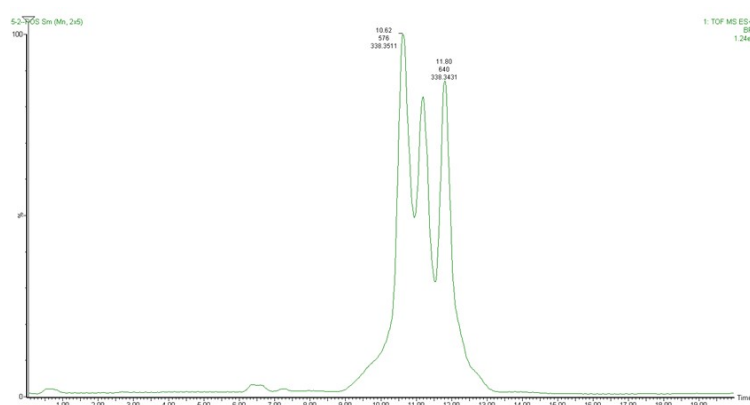


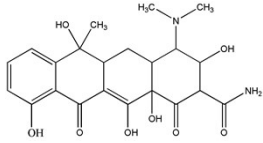
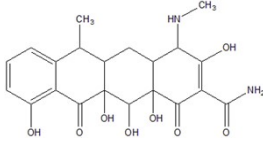
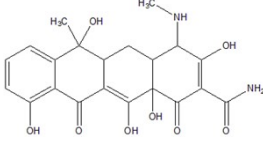
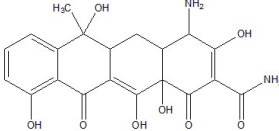
**Fig. S8** The total ion chromatogram of HPLC-MS

**Table. S1** The ions leaching before and after the reaction

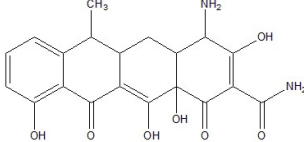
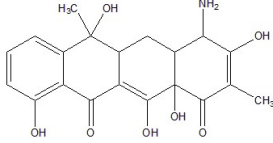
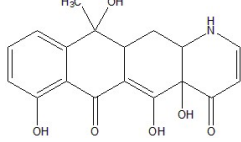
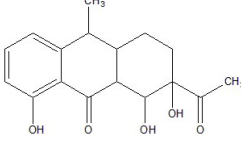
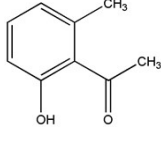
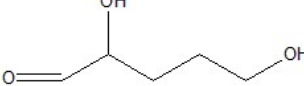
ion species	Pre-reaction concentration	Post-reaction concentration
Ni	0.51	0.25
Fe	0.68	0.14

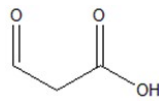
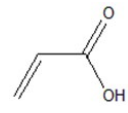
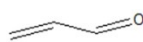
**Table. S2** The main intermediates of TC-HCl

m/z	分子式	结构式
-----	-----	-----

445	$C_{22}H_{24}O_8N_2$	
431	$C_{21}H_{22}O_8N_2$	
431	$C_{21}H_{22}O_8N_2$	
417	$C_{20}H_{20}O_8N_2$	

( continuation sheet. S2 )

m/z	分子式	结构式
399	$C_{20}H_{19}O_7N_2$	
388	$C_{20}H_{21}O_7N$	
344	$C_{18}H_{21}O_6N$	
305	$C_{17}H_{19}O_5$	
135	$C_9H_{10}O_2$	
104	$C_5H_{10}O_3$	

89	$C_3H_4O_3$	
73	$C_3H_4O_2$	
57	$C_3H_4O$	

**Table. S3** Condensed Fukui functions and condensed dual descriptors

Atom	q(N)	q(N+1)	q(N-1)	CDD
1(C)	-0.0261	-0.0729	0.0075	0.0132
2(C)	-0.0649	-0.0856	0.0028	-0.047
3(C)	-0.0033	-0.0227	0.0165	-0.0003
4(C)	-0.0444	-0.0521	-0.0066	-0.0302
5(C)	0.0985	0.0754	0.1409	-0.0194
6(C)	-0.0551	-0.085	-0.0071	-0.0182
7(C)	0.0862	0.0845	0.0883	-0.0003
8(C)	-0.0184	-0.0211	-0.0147	-0.0009
9(C)	-0.0401	-0.0578	-0.0077	-0.0147
10(C)	0.136	0.078	0.1446	0.0493
11(C)	-0.0503	-0.0539	-0.0476	0.0009
12(C)	-0.0239	-0.0252	-0.0226	0
13(C)	0.0662	0.0574	0.0722	0.0029
14(C)	0.0901	0.0598	0.1209	-0.0004
15(C)	0.0261	0.0202	0.0286	0.0034
16(C)	0.1372	0.0809	0.148	0.0455
17(C)	-0.0636	-0.0816	-0.0552	0.0097
18(C)	0.1358	0.0865	0.1423	0.0429
19(C)	0.1511	0.1436	0.1748	-0.0162
20(C)	-0.0909	-0.0969	-0.0844	-0.0005
21(O)	-0.1869	-0.2181	-0.1029	-0.0528
22(O)	-0.2158	-0.2786	-0.1934	0.0403
23(O)	-0.1755	-0.1983	-0.1431	-0.0096
24(O)	-0.2077	-0.2619	-0.1902	0.0367



25(O)	-0.2018	-0.2259	-0.1845	0.0068
26(O)	-0.2123	-0.2168	-0.2015	-0.0062
27(O)	-0.3185	-0.3465	-0.2255	-0.065
28(N)	-0.1487	-0.1622	-0.1191	-0.0161
29(N)	-0.0625	-0.0655	-0.0593	-0.0002
30(C)	-0.0336	-0.0409	-0.0296	0.0033
31(C)	-0.0389	-0.0439	-0.0355	0.0017
32(O)	-0.1267	-0.1719	-0.1096	0.0281
33(H)	0.0447	0.0177	0.0709	0.0008
34(H)	0.033	0.017	0.0607	-0.0118
35(H)	0.0466	0.0246	0.0745	-0.0059
36(H)	0.0296	0.0192	0.0411	-0.0012
37(H)	0.031	0.0258	0.0351	0.0011
38(H)	0.0293	0.0172	0.0388	0.0026
39(H)	0.0344	0.0253	0.0399	0.0037
40(H)	0.0455	0.0289	0.0517	0.0104

( continuation sheet. S3 )

Atom	q(N)	q(N+1)	q(N-1)	CDD
41(H)	0.0317	0.0209	0.0405	0.002
42(H)	0.0327	0.0246	0.0411	-0.0002
43(H)	0.0318	0.0242	0.0436	-0.0043
44(H)	0.1148	0.1036	0.1339	-0.0079
45(H)	0.1236	0.1114	0.1357	0.0001
46(H)	0.1452	0.132	0.154	0.0044
47(H)	0.1499	0.139	0.1588	0.002
48(H)	0.1249	0.1059	0.1454	-0.0014
49(H)	0.0926	0.0863	0.1061	-0.0072
50(H)	0.026	0.0204	0.0276	0.0041
51(H)	0.0415	0.0274	0.0519	0.0037
52(H)	0.0379	0.03	0.0419	0.0039
53(H)	0.0268	0.0214	0.0292	0.0031
54(H)	0.0365	0.0351	0.0373	0.0006
55(H)	0.0379	0.023	0.0487	0.0042
56(H)	0.1348	0.1184	0.1446	0.0066

